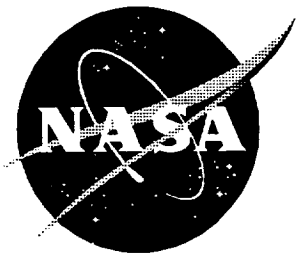

NASA Contractor Report 4702

Implementation of Algebraic Stress Models in a General 3-D Navier-Stokes Method (PAB3D)

Khaled S. Abdol-Hamid

Contract NAS1-19831
Prepared for Langley Research Center

December 1995

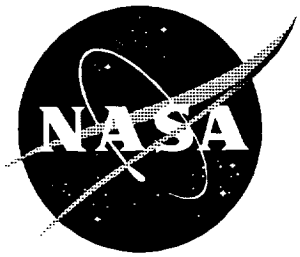

NASA Contractor Report 4702

Implementation of Algebraic Stress Models in a General 3-D Navier-Stokes Method (PAB3D)

Khaled S. Abdol-Hamid
Analytical Services & Materials, Inc.• Hampton, Virginia

National Aeronautics and Space Administration
Langley Research Center • Hampton, Virginia 23681-0001

Prepared for Langley Research Center
under Contract NAS1-19831

December 1995

Printed copies available from the following:

NASA Center for AeroSpace Information
800 Elkridge Landing Road
Linthicum Heights, MD 21090-2934
(301) 621-0390

National Technical Information Service (NTIS)
5285 Port Royal Road
Springfield, VA 22161-2171
(703) 487-4650

Implementation of Algebraic Stress Models in a General 3-D Navier-Stokes Method (PAB3D)

Khaled S. Abdol-Hamid
Analytical Services and Materials, Inc.
Hampton, VA

Abstract

A three-dimensional multiblock Navier-Stokes code, PAB3D, which was developed for propulsion integration and general aerodynamic analysis, has been used extensively by NASA Langley and other organizations to perform both internal (exhaust) and external flow analysis of complex aircraft configurations. This code was designed to solve the simplified Reynolds Averaged Navier-Stokes equations. A two-equation k-ε turbulence model has been used with considerable success, especially for attached flows. Accurate predicting of transonic shock wave location and pressure recovery in separated flow regions has been more difficult. Two algebraic Reynolds stress models (ASM) have been recently implemented in the code that greatly improved the code's ability to predict these difficult flow conditions. Good agreement with Direct Numerical Simulation (DNS) for a subsonic flat plate was achieved with ASMs developed by Shih, Zhu, and Lumley and Gatski and Speziale. Good predictions were also achieved at subsonic and transonic Mach numbers for shock location and trailing edge boattail pressure recovery on a single-engine afterbody/nozzle model.

Introduction

CFD methods along with accurate turbulence models are required to predict aerodynamic effects at transonic conditions. Accurate prediction of pressure distribution and skin friction coefficient is of paramount importance to the design of aerodynamic configurations. Accurate predictions of boundary layer structure and flow separation by CFD methods are also very critical.

It is widely accepted that the computational economy of two-equation turbulence models (ref. 1) offers a reasonable compromise for computing practical flow problems. The theoretical advantages of these models over algebraic models are the incorporation of turbulence history-dependent non-local effect (through the convection and viscous diffusion of the Reynolds stress) which are known to play an important role in determining the turbulence structure in complex flows. In the standard two-equation k-ε turbulence model, transport equations are carried for kinetic energy and dissipation (ref. 1). The k-ε equations can be applied to the near wall region as well as far away from wall boundaries. For regions of the flow far away from solid boundaries, the high Reynolds number form of the model can be used while wall damping functions must be used when applying the model near wall boundaries.

Reynolds Stress models (refs. 2 & 3) have the potential of producing more accurate turbulent simulation as compared with two-equation turbulence models. However, numerical calculations using the more advanced Reynolds Stress models require the solution of transport equations for each individual component of the Reynolds stress tensor (five more equations) besides solving the Navier-Stokes equations. This approach requires tremendous computational time when solving three-dimensional (3-D) flow problems. Moreover, the transport equations for the second-order models require closure approximation for higher-order turbulence correlation that has uncertain physical foundations.

As an alternative to Reynolds Stress turbulence models, Shih et al.[4] and Gatski and Speziale[5] developed algebraic forms of the Reynolds stress model, which broadened the range of applicability of the existing linear models (k-ε for example) while maintaining most of their popular features (such as reduction to mixing layer theories for thin shear flows and the possibility of implementation in

existing Navier-Stokes codes without substantially increasing the computational time). These algebraic stress models (ASM) were developed by making an asymptotic expansion subject to constraints of dimensional and tensorial invariance, realizability, and material frame indifference. The resulting ASM models showed substantially improved predictions in incompressible turbulent channel flows and yielded normal Reynolds-stress differences that gave rise to secondary flows in complex flows.

In the present research work, the ASM models developed by Shih, Zhu, and Lumley (SZL) and Gatski and Speziale (GS) were implemented and tested in the CFD code PAB3D. The GS algebraic stress model uses coefficients derived from the Sarker, Gastki, and Speziale[5] (SSG) Reynolds Stress model. PAB3D is a general purpose, 3-D, multiblock Navier-Stokes code described and applied in ref. 1. The flow solver contains the Baldwin-Lomax[6] turbulence model and a two-equation k-ε turbulence model with various near wall damping functions. The two ASM models identified above were implemented for the present study to resolve flow field anisotropy. The code has a built in performance module to compute various quantities such as lift, drag, thrust, and discharge coefficient. During a typical numerical simulation, these quantities are constantly monitored to assess the performance of the propulsion system under consideration.

Computed results using ASM are compared with published experimental data at several levels of increasing flow complexity. The geometries considered in the present study are a subsonic flat plate[7], a transonic axisymmetric afterbody[8], and a supersonic square duct[9]. The flat plate was selected because it is the simplest of all the geometries for which experimental and direct numerical simulation[10] (DNS) data are available. The axisymmetric afterbody represents the next level of flow complexity because this case contains a separated flow region. The separation is generated by either an adverse pressure gradient or a shock boundary layer interaction. The square duct case provides a simple, full 3-D test case with complex flow structure. In this case, secondary flow is generated by the anisotropy of the normal stress components.

Symbols and Abbreviations

C_1, C_2, C_3, and C_4	model constants for the GS Algebraic Stress model
$C_{\varepsilon 1}$, and $C_{\varepsilon 2}$	model constants for the k-ε turbulence model
C_μ	turbulence viscosity coefficient for the k-ε model . .09
Cp	pressure coefficient
D	duct width, cm.
k	turbulent kinetic energy, Pa.
l	length of the axisymmetric model
n	normal distance from the wall, cm.
S_{ij}	Strain component, 1/sec
U_{ij}	$\frac{\partial u_i}{\partial x_j}$, velocity gradient, 1/sec
$y^+=n^+$	law-of-the-wall coordinate , $\frac{n\sqrt{\rho_w \tau_w}}{\mu_w} = \frac{n\rho_w u_\tau}{\mu_w}$
Re_x	Reynolds number based on streamwise distance from the plate leading edge, $u_\infty \rho_\infty x/\mu_\infty$.
u,v,w	velocity components in the (x,y,z) directions, m/sec.
u^+	law-of-the wall coordinate, $\frac{u}{u_\tau} = \frac{Re_c}{n^+}$
u_τ	friction velocity, $\sqrt{\tau_w / \rho}$
x,y,z	spatial coordinates, cm.
δ	Kronecker delta and boundary layer thickness
κ	von Karman constant.
ε	turbulent energy dissipation
γ	ratio of specific heat, 1.4.
μ	dynamic viscosity coefficient, m^2/sec.
ν	kinematic viscosity coefficient, m^2/sec.
ρ	density, kg/m^3
τ_{ij}	Reynolds stress components.
τ_w	wall shear stress, $\mu \frac{\partial u}{\partial n}\Big\|_w$
Ω	vorticity
(ξ, η, ζ)	generalized coordinates as functions of (x,y,z)

Superscripts

L	laminar
T	turbulent

Abbreviations

ASM	algebraic stress model
DNS	direct numerical simulation
GS	Gatski and Speziale algebraic stress model
SSG	Sarker, Gatski, and Speziale Reynolds stress model
SZL	Shih, Zhu and Limley algebraic stress model
k-ε	k-epsilon model - Jones-Launder wall damping
V13	Version 13 of PAB3D code

Computational Procedure

Code Structure

Figure 1 presents a sketch of the logical structure of the PAB3D code. This code solves the Reynolds Averaged Navier-Stokes (RANS) equations, along with several different forms of a two-equation turbulence model, written in a general 3-D form. It requires 15 words per grid point to compute laminar or turbulent flows using algebraic turbulence models and 20 words per grid point to compute turbulent flows using a two-equation turbulence model. The code speed is 33μs and 43μs per grid point (Cray 2 time) for solving laminar and turbulent flows, respectively. The convective (inviscid) terms of the transport equations (RANS and turbulence equations) are simulated using state-of-the-art upwind schemes[1]. The viscous and diffusion terms in these equations are evaluated using a central difference scheme. The two-equation turbulence model equations are uncoupled from the RANS equations and solved with a different time step. Different near-wall, compressibility and damping coefficients can be used with any of the two-equation turbulence model options available in the code. Recently, several different forms of Algebraic Reynolds Stress turbulence models (ASM)[4,5] have been implemented in the PAB3D code (V13). The code utilizes post- and pre-processing software packages for manipulation of the computational grids, solutions, and the creation of the patched block interface data base. A 3-D performance package is utilized to calculate aerodynamic quantities such as nozzle discharge coefficient and thrust ratio for exhaust systems, and lift and drag coefficient for aerodynamic bodies.

Eddy Viscosity Turbulence Models

In most 3-D Navier-Stokes codes, the stress components are modeled as:

$$\tau_{ij} = \tau_{ij}^{L} + \tau_{ij}^{T}$$

Where, τ is calculated with the eddy viscosity formulation through the Boussinesq's hypothesis and following Kolmogorov:

$$\tau_{ij}^{T} = A^{T}\delta_{ij} - 2\mu_{\tau}S_{ij}$$

$$\tau_{ij}^{L} = A^{L}\delta_{ij} - 2\mu_{L}S_{ij}$$

where,

$$S_{ij} = \frac{1}{2}(U_{i,j} + U_{j,i})$$

$$A^{T} = \frac{2}{3}(\rho k + \mu_{T}S_{kk})$$

$$A^{L} = \frac{2}{3}\mu_{L}S_{kk}$$

$$\mu_{T} = f_{\mu}C_{\mu}\frac{k^{2}}{\varepsilon}$$

and, f_{μ} is an empirical function and C_{μ} is set to a value of .09 for the standard k-ε model (linear model). K is the turbulent kinetic energy and ε is the rate of dissipation. Despite the current popularity of the k-ε turbulence model, it still shares a common deficiency with the mixing length algebraic turbulence models, i.e. the Boussinesq eddy viscosity hypothesis. It is well known that these models give inaccurate prediction of normal Reynolds stress differences, which makes the eddy viscosity models incapable of simulating complex flows. In the above formulation, stress components are directly related to the rate of strain S after dropping the k term. This simplifies the implementation of the two equation turbulence model in most 3-D Navier-Stokes codes due to the eddy viscosity form as described in Ref. 1.

Algebraic Stress Models

The use of the algebraic stress models (ASMs) is not as straight forward as the implementation of lower level turbulence models (including the two-equation linear turbulence model). Because of the nonlinear relation between stress and the velocity gradients, turbulence stresses must be evaluated at the cell faces instead of the cell centers. The six stress components (laminar and turbulent) are computed for each cell. The full 3-D codes require the calculation of each stress component at the six faces of each cell for a total of 36 values. Fortunately, in

most cases, the viscous diffusion terms can only be evaluated in one or two directions, mostly due to grid restrictions. This reduces the number of variables to 12 or 24.

In the present study, two ASM models (SZL and GS) were implemented in the PAB3D code. SZL[4] developed a new Reynolds stress algebraic equation model using a general turbulent constitutive relation (Shih and Lumley[11]). In this development, the constraints based on rapid distortion theory and realizability are imposed. In this model, turbulent stress components are composed of linear and nonlinear parts as follows:

$$\tau_{ij}^{T} = \tau_{ij}^{T(l)} + \tau_{ij}^{T(n)}$$

$$\tau_{ij}^{T(l)} = A\delta_{ij} - 2\mu_{\tau}S_{ij}$$

$$\tau_{ij}^{T(n)} = 2\beta\frac{k^3}{\varepsilon^2}(\Omega_{ik}^{*}S_{kj}^{*} - S_{ik}^{*}\Omega_{kj}^{*})$$

where,

$$\beta = \frac{\sqrt{1-9C_{\mu}^{2}(\frac{S^{*}k}{\varepsilon})^{2}}}{1+6\frac{S^{*}k}{\varepsilon}\frac{\Omega^{*}k}{\varepsilon}}$$

$$C_{\mu} = \frac{1}{6.5+A_{s}^{*}\frac{U^{*}k}{\varepsilon}}$$

$$A_{s}^{*} = \sqrt{6}\cos(\phi)$$

$$\phi = \frac{1}{3}\cos^{-1}(\sqrt{6}W^{*})$$

$$S^{*} = \sqrt{S_{ij}^{*}S_{ij}^{*}}, \quad S_{ij}^{*} = S_{ij} - \frac{1}{3}\delta_{ij}S_{kk}$$

$$\Omega^{*} = \sqrt{\Omega_{ij}^{*}\Omega_{ij}^{*}},$$

$$\Omega_{ij}^{*} = \Omega_{ij} = \frac{1}{2}(U_{i,j} - U_{j,i}) = -\Omega_{ji}$$

$$W^{*} = \frac{S_{ij}^{*}S_{jk}^{*}S_{ki}^{*}}{(S^{*})^{3}} \text{ and } U^{*} = \sqrt{S_{ij}^{*}S_{ij}^{*} + \Omega_{ij}^{*}\Omega_{ij}^{*}}$$

GS[5] describes the relationship between the new explicit algebraic stress models and anisotropic eddy viscosity models in reference 5. The GS form of the explicit algebraic stress model was implemented in PAB3D as follows:

$$\tau_{ij}^{T(n)} = C_\mu \frac{k^3}{\varepsilon}[\beta_1(\Omega_{ik}S_{kj} - S_{ik}\Omega_{kj}) + \beta_2(S_{ik}S_{kj} - \tfrac{1}{3}S_{mn}S_{mn}\delta_{ij})]$$

$$C_\mu = \frac{3(1+\eta^2)\alpha}{3+\eta^2+6\eta^2\zeta^2+6\zeta^2}$$

$$\beta_1 = g(2-C_4) \text{ and } \beta_2 = 2g(2-C_3)$$

$$\alpha = g(\tfrac{4}{3}-C_2)$$

$$\eta^2 = S_{ij}^* S_{ij}^*, \zeta^2 = \Omega_{ij}^* \Omega_{ij}^*$$

$$S_{ij}^* = \frac{k}{2\varepsilon} g(2-C_3)S_{ij}$$

$$\Omega_{ij}^* = \frac{k}{2\varepsilon} g(2-C_4)\Omega_{ij}$$

$$g = \frac{1}{\left(\frac{C_1}{2}+\frac{C_{\varepsilon 2}-1}{C_{\varepsilon 1}-1}-1\right)}$$

$$C_1 = 3.4 + \frac{C_{\varepsilon 2}-1}{C_{\varepsilon 1}-1}, C_2 = 0.368, C_3 = 1.25, C_4 = 0.4$$

Results and Discussion

Because of the complex nature of the flow discussed in this paper, it was essential to maintain appropriate grid spacing near solid boundaries to ensure appropriate near wall behavior of k and ε. For the current study, y^+ of the first point located off the wall was less than one and the grid was stretched in the normal direction using an exponential grid stretching formula. Approximately 16 points were placed normal to the walls to resolve the boundary layer. The rest of the points in the normal direction were distributed uniformly between the edge of the boundary layer and the farfield or the symmetry boundary.

Subsonic Flow Over a Flat Plate

The first test case considered in the present study was subsonic flow over a flat plate (ref. 7). Four physical properties of flow over a flat plate were chosen to evaluate the accuracy of the different forms of the two-equation and algebraic stress models. These parameters were evaluated at R_θ of 1420. The four properties are:

1) u^+ (normalized velocity)

$$u^+ = u^* / u_\tau$$

$$u_\tau = \int_0^{u_\infty} \sqrt{\rho / \rho_w}\, du$$

This parameter is a standard variable in evaluating turbulence model accuracy. Laminar sublayer, buffer, and turbulent regions should be clearly defined during this evaluation.

2) k^+ (normalized turbulence kinetic energy)

$$k^+ = k / u_\tau^2$$

3) $u'v'^+$ (normalized shear stress)

$$u'v'^+ = u'v' / u_\tau^2 = \tau_{12} / u_\tau^2$$

4) u'^{+2}, v'^{+2}, w'^{+2} (normalized normal stress components), for example

$$u'^{+2} = u'^2 / u_\tau^2 = \tau_{11} / u_\tau^2$$

These parameters were selected to show three-dimensionality of normal stress components for a two-dimensional (2-D) flow case.

Figure 2 shows the comparison of the calculated boundary layer parameters with DNS[10] and experimental data. In figure 2a, the standard Jones and Launder two-equation turbulence model shows substantial deficiencies in predicting any of the four parameters. In predicting the normalized velocity, u^+, the flow transitioned from a laminar sublayer directly to a fully turbulent region without going through a buffer region. The model under predicted the k+ peak by about 20 percent. Also, the peak shear stress was under predicted by at least 10 percent. As expected, the turbulence model did not predict the three-dimensionality of the normal stress components due to the two-equation k-ε turbulence model assumptions of a linear relation between stress and strain.

The second turbulence model evaluated is the SZL algebraic stress model. Figure 2b shows the evaluation of this turbulence model in prediction of the four properties. The u+ is in excellent agreement with experimental as well as the

theoretical data. All of the flow regions are well defined in this prediction. The model accurately predicted the k+ peak as compared with the DNS data. Similarly, the shear stress peak is more accurately predicted although somewhat low. The model also shows the anisotropy of the three normal stress components.

The algebraic stress model based on the SSG coefficients are compared with the data in figure 2c. This model provides the best agreement with DNS and experimental data when compared with the other two turbulence models. Correct kinetic energy and shear stress peaks and the general features of all four parameters are captured well. However, this turbulence model required a smaller time step to avoid divergence of the solution and it needed 20 percent more iterations to achieve similar solution accuracy as the SZL model.

Transonic Axisymmetric Afterbody/Nozzle

The second test case considered was an axisymmetric afterbody/nozzle with a constant diameter cylinder representing a solid jet exhaust plume simulation (see ref. 8). This configuration, although axisymmetric, can involve solutions where all three dimension components of Reynolds stress are non-zero and unequal. Mach numbers of 0.6, 0.85 and 0.9 were the selected freestream flow conditions for this test case. For this configuration, a separated flow region occurs on the nozzle boattail through different flow mechanisms depending on freestream Mach number. At M = 0.60, separation is caused by an adverse pressure gradient. The separated flow regions at Mach numbers of 0.85 and 0.90 occur due to a shock/boundary-layer interaction.

Figure 3 shows the comparison between the experimental data (ref. 8) for this test case and two different turbulence model predictions. The standard k-ε model and the GS form of the algebraic Reynolds stress model are shown for this prediction. There was little difference between results using the SZL (not shown) or GS models except for convergence history. All the calculations agree well with the data up to the separated flow region or the location of the shock. In general, the standard (linear) two-equation turbulence model overpredicted the pressure recovery on the afterbody by at least 40 percent as shown in figure 3a. For the Mach = 0.90 case, the linear turbulence model predicted the shock location downstream of the data. The GS form of the algebraic Reynolds stress (nonlinear)

model accurately predicted the pressure recovery in the separated region as well as the calculated shock location (see figure 3b).

Supersonic Square Duct

The final test case geometry was a square duct (ref. 9). Numerical calculations were carried out for supersonic flow through square duct using linear and SZL k-ε turbulence models. The duct Mach number was 3.9 and the unit Re was 1.2 million/m. Figure 4 shows the cross flow velocity patterns computed using the two different turbulence models at X = 20, 30, 40 and 50. Dramatically improved results are obtained using the SZL model as shown in figure 4b. Similar to the experimental results reported in reference 9, the SZL computations clearly show that the secondary flows (vortices) are symmetrical about the diagonal and rotate in opposite directions. These vortices are essentially driven by the gradients of the Reynolds stresses which transport net momentum towards the corner of the duct and cannot be simulated by the linear models. The computed cross flow velocity vectors using the SZL turbulence model are in good agreement with the experimentally observed patterns. In contrast, the linear model predicts a unidirectional flow due to the inability of the turbulence model to represent the flow physics.

Concluding Remarks

An investigation of the effect of using standard k-ε and algebraic Reynolds stress turbulence models on the computed flow field of several different aerodynamic configurations was conducted. The computed results were compared with the available computations, experimental, and theoretical data bases. The geometries considered in the present study were a flat plate, a transonic axisymmetric afterbody and supersonic flow through a square duct.

The flat plate test case was selected because it is the simplest of all the 2-D geometries which show the three-dimensionality of the normal turbulent stress components. The results obtained using either the SZL or the GS form of the explicit algebraic Reynolds stress (ASM) turbulence model were more accurate and consistent than the standard (linear) k-ε turbulence model. The ASM

turbulence model accurately predicted the turbulent kinetic energy and shear stress peaks as well as the anisotropy of the normal stress components.

The axisymmetric afterbody geometry represented the next level flow complexity because this case contains separated flow regions driven by either an adverse pressure gradient or a shock/boundary-layer interaction. The algebraic Reynolds stress turbulence model generally provided accurate predictions of the pressure recovery in separated flow regions whereas the standard k-ε turbulence model overpredicted the pressure recovery in these regions. In addition, the ASM turbulence model generally provided better predictions of shock location.

For the test case of square duct geometry, a secondary flow structure developed in directions perpendicular to the main flow. The ASM results clearly showed that the secondary flows (vortices) were symmetrical about the duct diagonal and rotate in opposite directions. These vortices are essentially driven by the gradients of the Reynolds stresses, which could not be simulated by the linear model.

This investigation provided significant insight into the applications of explicit algebraic Reynolds stress turbulence models in predicting attached and separated flows. The results of this investigation support a high level of confidence in using these advanced turbulence models for more complex aerodynamic configurations.

REFERENCES

1. Abdol-Hamid, K. S.; Lakshmanan, B.; and Carlson, J. R.: Application of a Navier-Stokes Code PAB3D with k-ε Turbulence Model to Attached and Separated Flows. NASA TP-3480, 1995.

2. Launder, B. E.; Reece, G. J.; Rodi, W.: Progress in the Development of a Reynolds Stress Closure. Journal of Fluid Mechanics, Vol. 68, 1975, pp. 537-566.

3. Sarkar, S.; and Lakshmanan, B.: Application of a Reynolds Stress Turbulence Model to the Compressible Shear Layer. AIAA Journal, Vol. 29, 1991, pp. 743-749.

4. Shih, Tsan-Hsing; Zhu, J.; and Lumley, John, L.: A New Reynolds Stress Algebraic Model. NASA TM-166644, ICOMP 94-8, 1994.

5. Gatski, T. B.; and Speziale, C. G.: On Explicit Algebraic Stress Models for Complex Turbulent Flows. NASA CR-189725, ICASE Report No. 92-58, 1992.

6. Baldwin, B. S.; and Lomax, H.: Thin Layer Approximation and Algebraic Model for Separated Turbulence Flows. AIAA 78-0257, 1978.

7. Wieghardt, K.; and Tillmann, W.: On the turbulent Friction Layer for Rising Pressure. NACA TM-1314, 1951.

8. Reubush, D. E.: Experimental Study of the Effectiveness of Cylindrical Plume Simulators for Predicting Jet-On Boattail Drag at Mach Numbers up to 1.3. NASA TN D-7795, 1974.

9. Gessner, F. B.; Ferguson, S. D.; and Lo, C. H.: Experiments on Supersonic Turbulent Flow Development in a Square Duct. AIAA Journal, Vol. 25, No. 5, May 1987, pp. 690-697.

10. Spalart, P. R.: Direct Simulations of Turbulent Boundary Layer up to $Re_\theta = 1410$. Journal of Fluid Mechanics, Vol. 187, pp. 61-98, 1988.

11. Shihm T, -H. and Lumley, J. L.: Remarks on Turbulent Constitutive Relations. Mathl. Comput. Modeling, Vol. No. 2, pp. 9-16, 1993

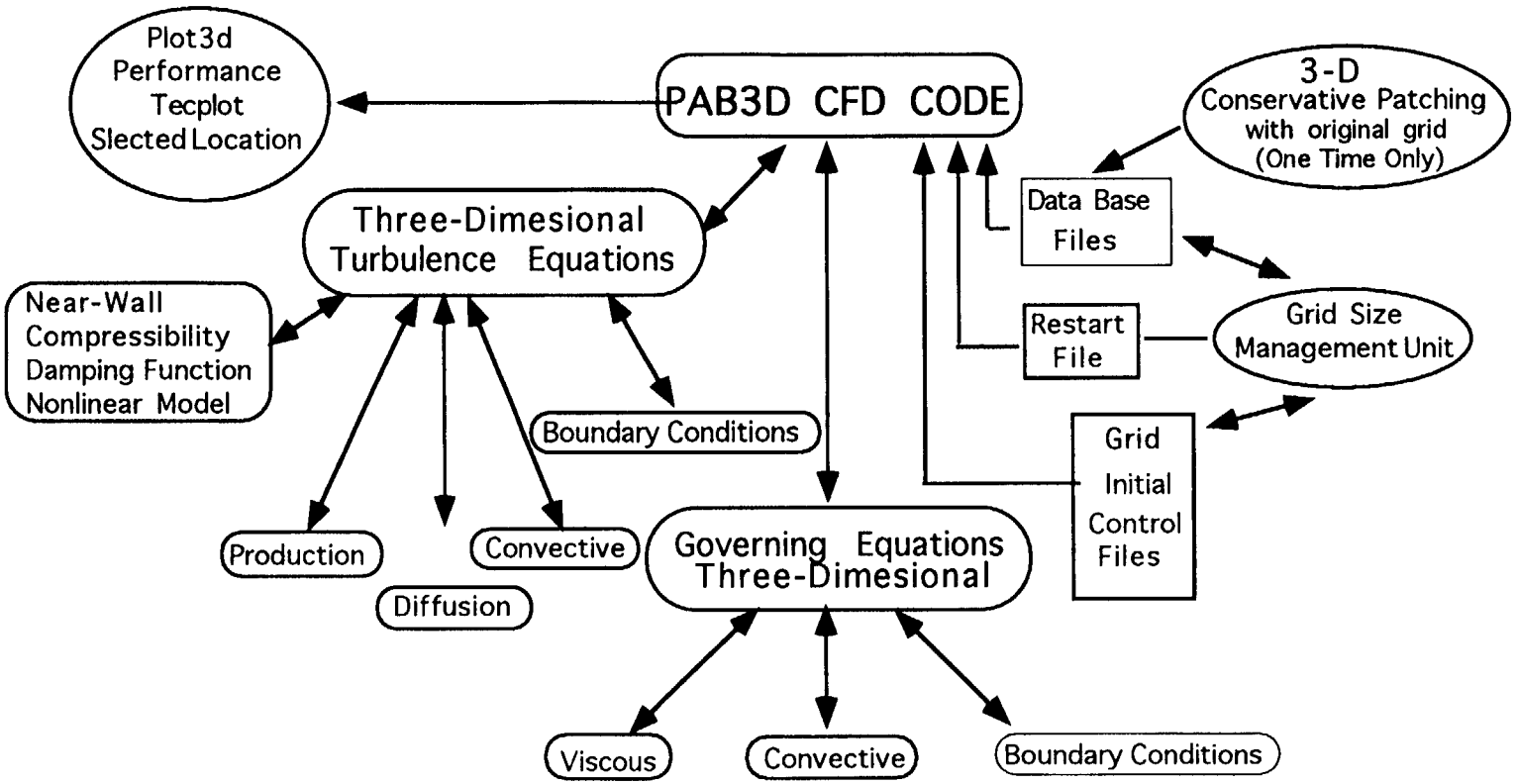

Figure 1. Sketch of Logical Structure of PAB3D code.

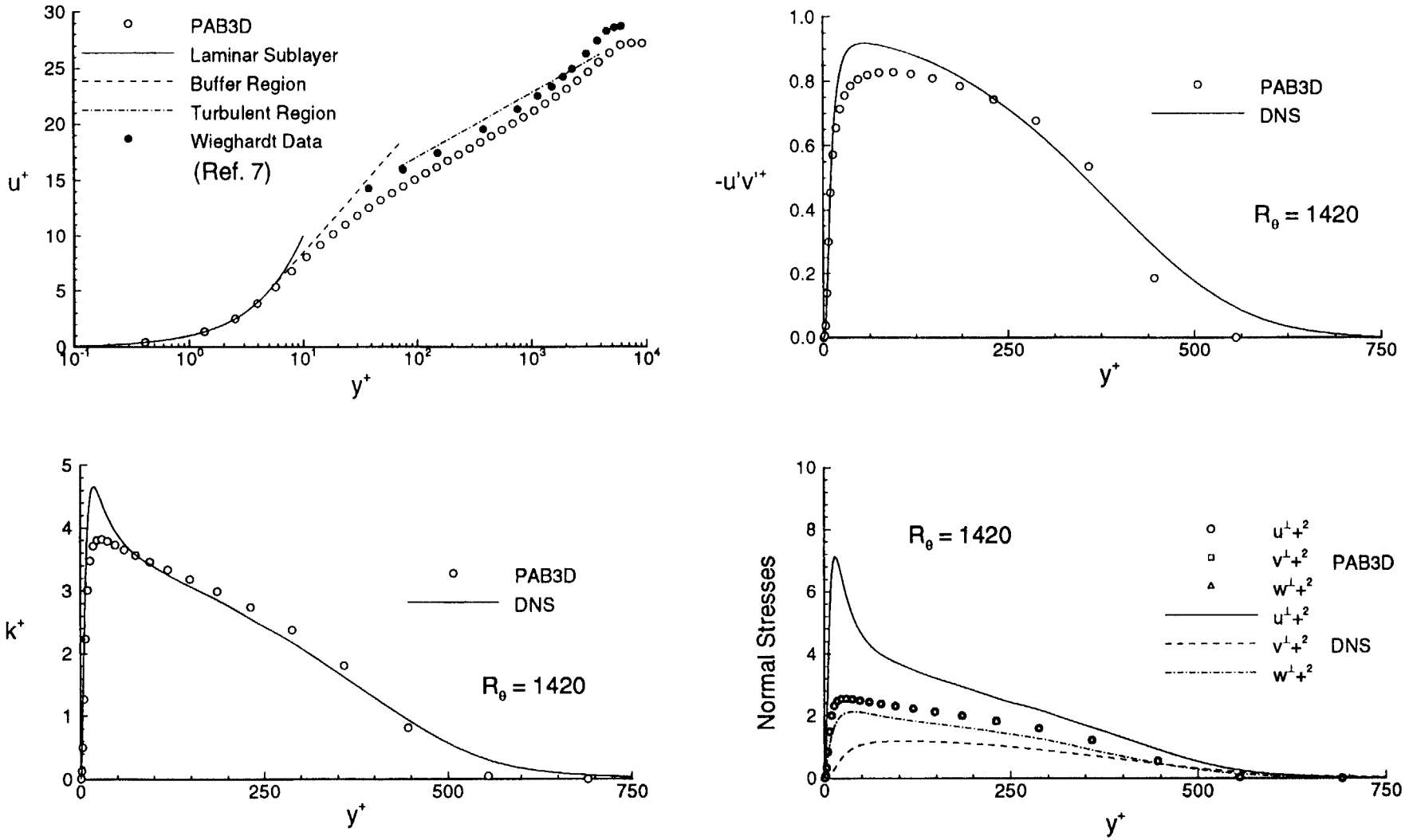

(a) Standard Jones & Launder 2-eqn. k-ε

Figure 2.- Comparison of calculated boundary layer parameters with DNS and data.

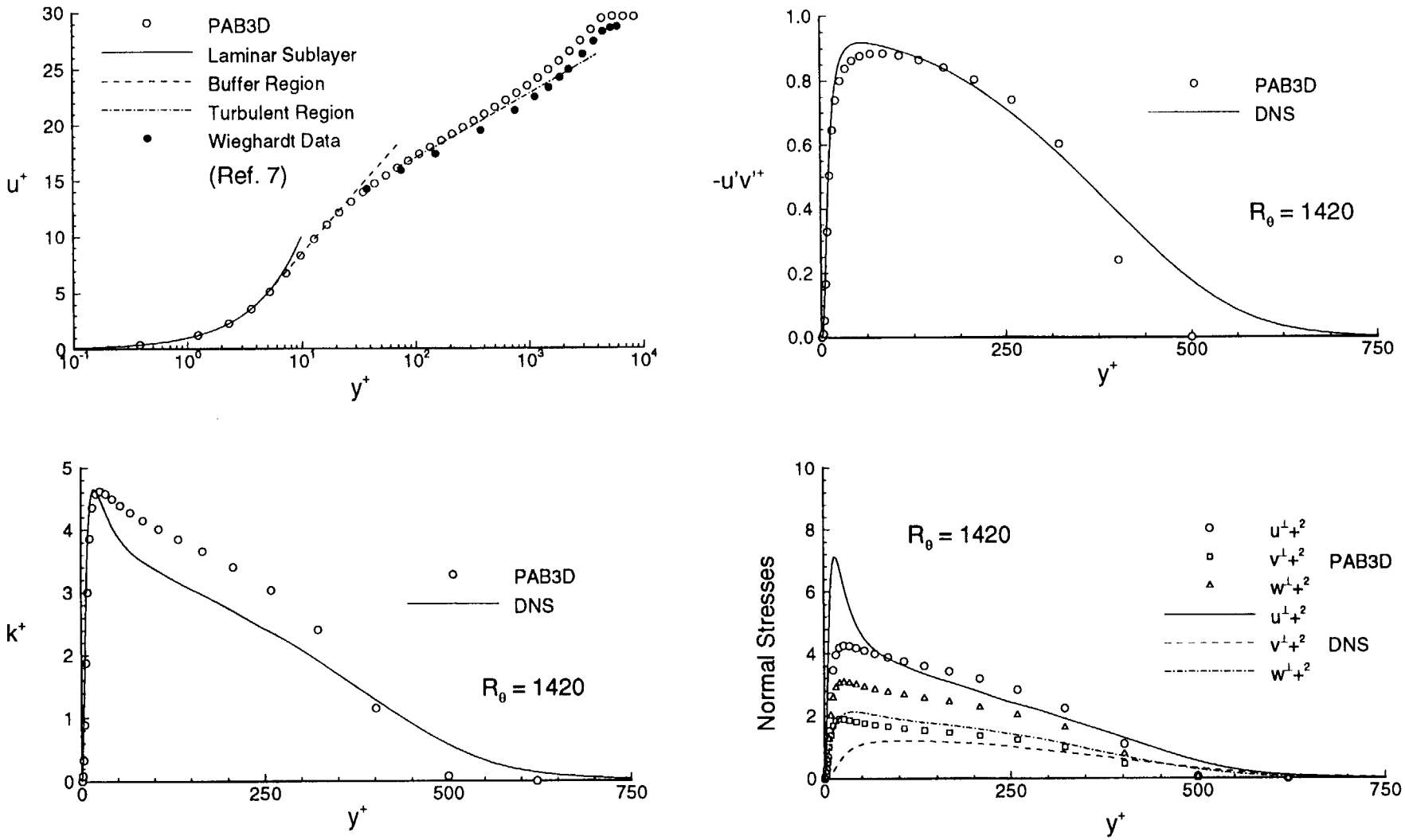

(b) Shih, Zhu & Lumley algebraic stress model.

Figure 2.- Continued.

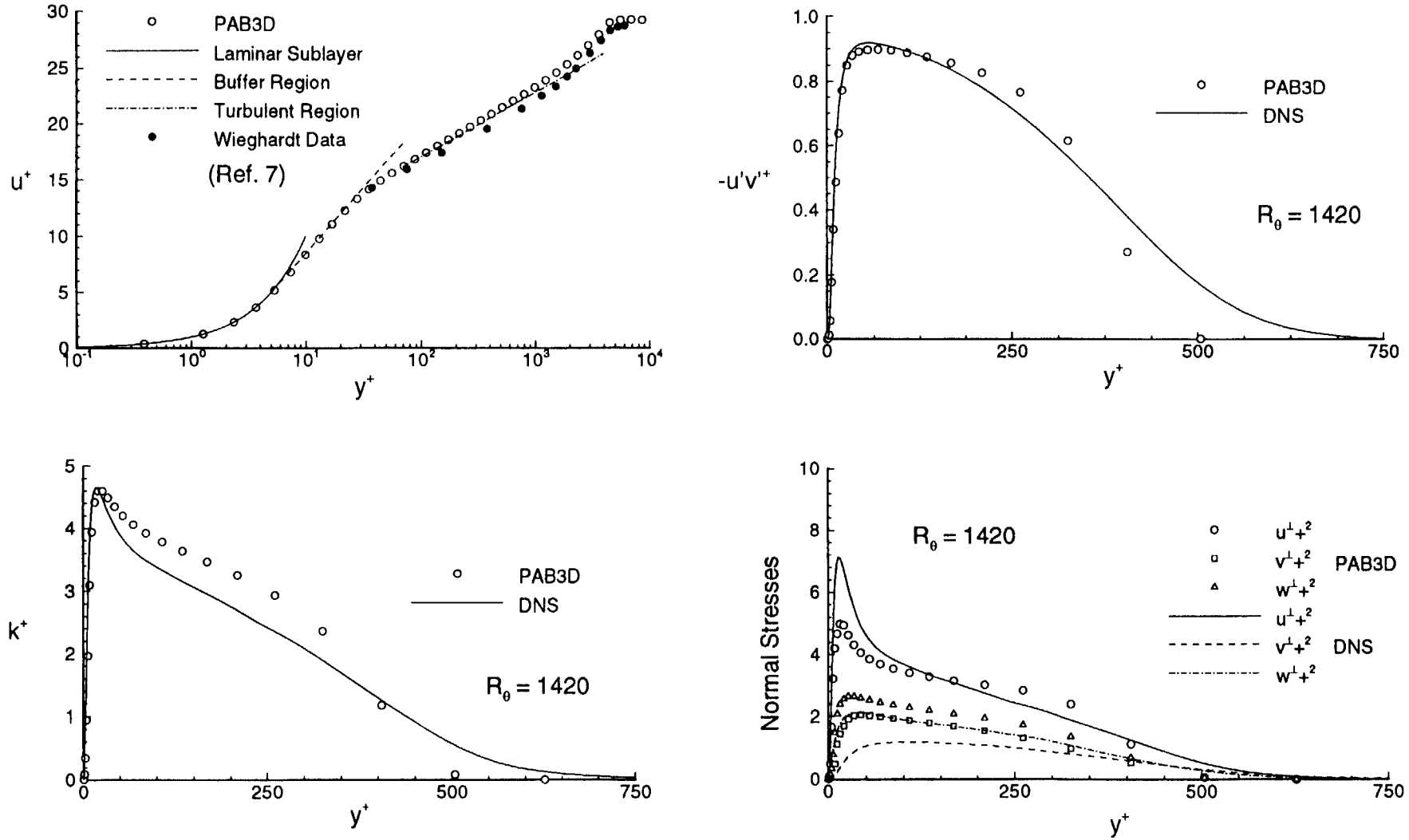

(c) Gatski & Speziale algebraic stress model.

Figure 2.- Concluded.

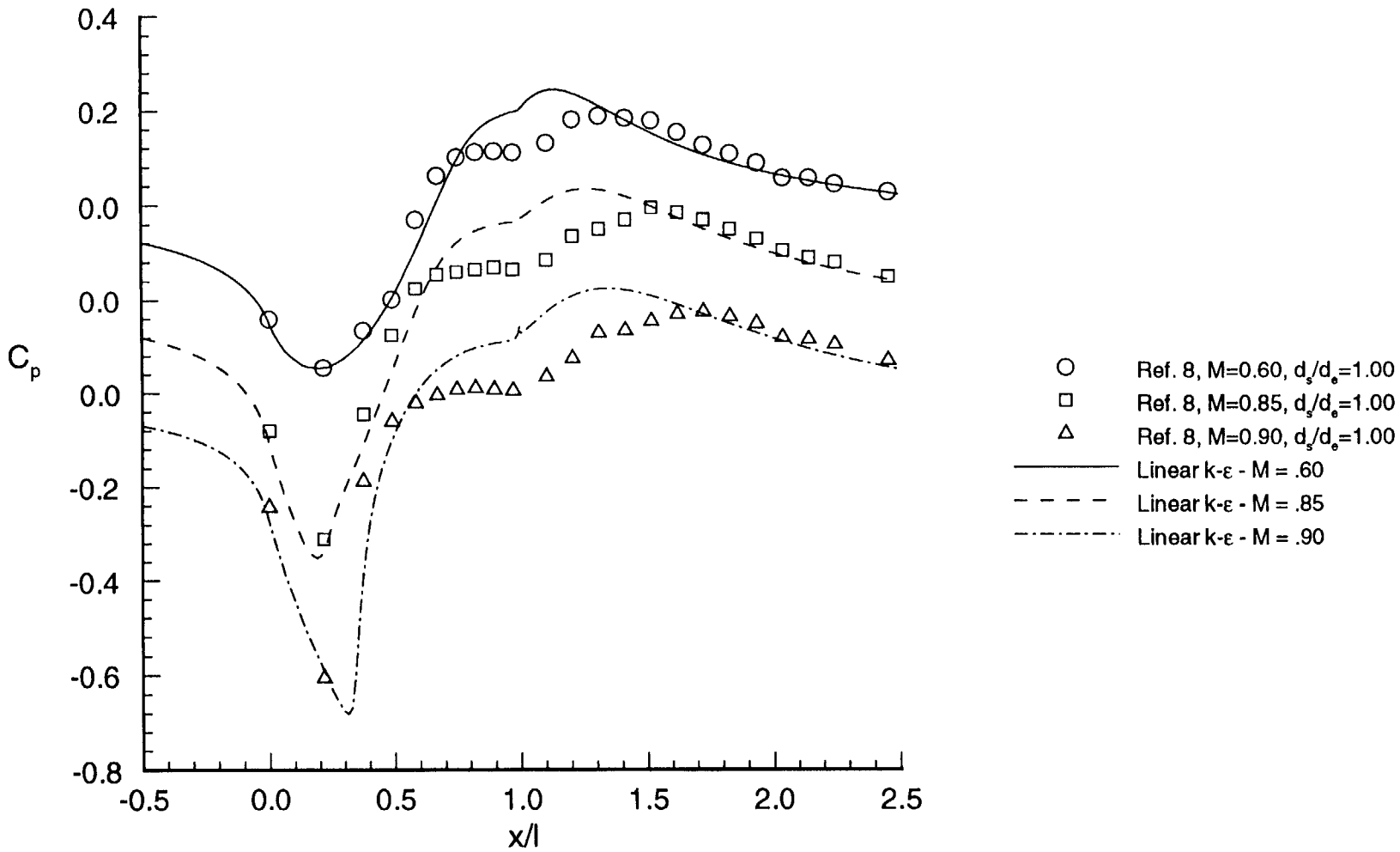

(a) standard Jones & Launder 2-eqn. k-ε

Figure 3. Experimental and predicted pressure distribution on axisymmetric afterbody with solid plume.

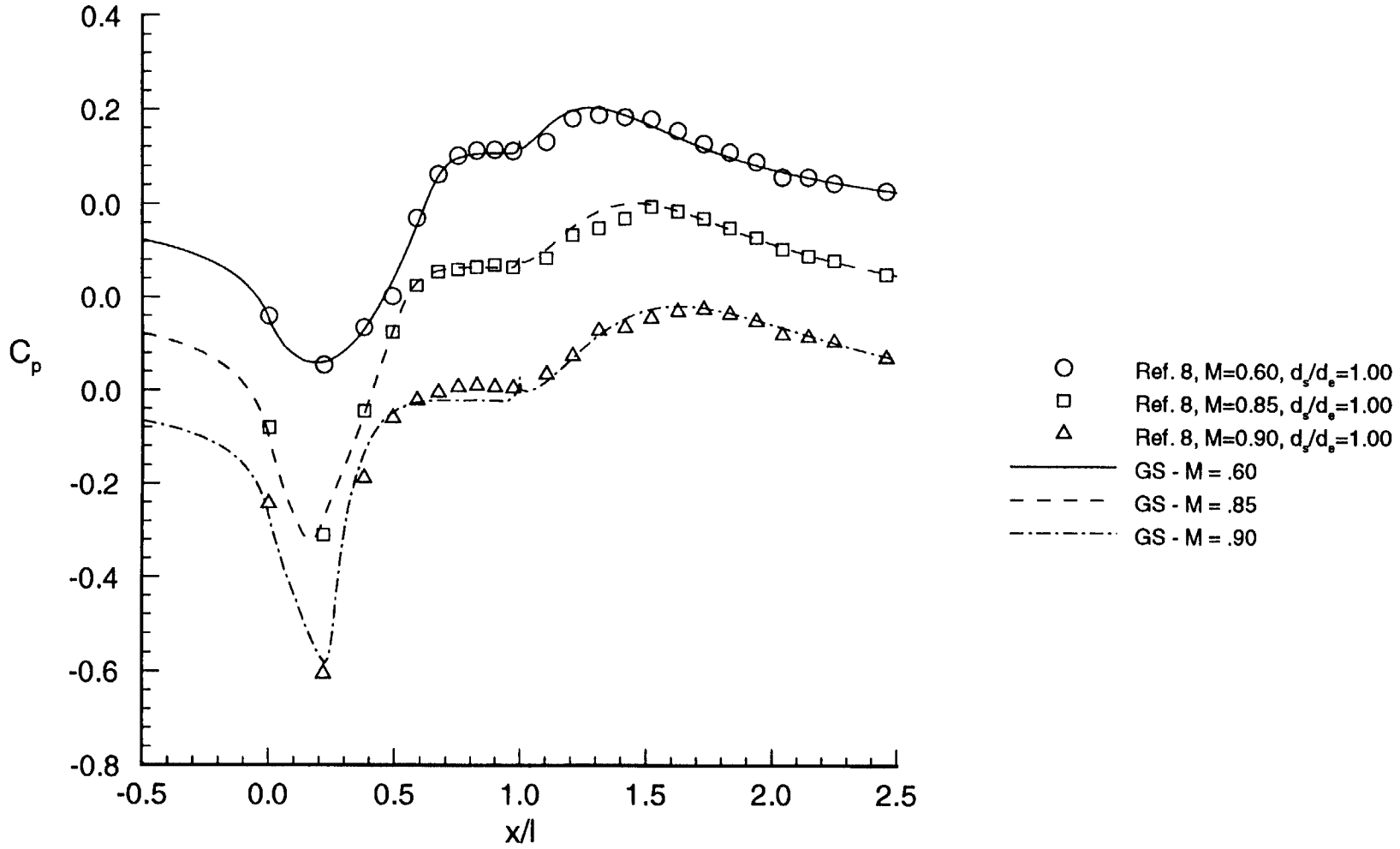

(b) Gatski & Speziale algebraic stress model.

Figure 3. Concluded

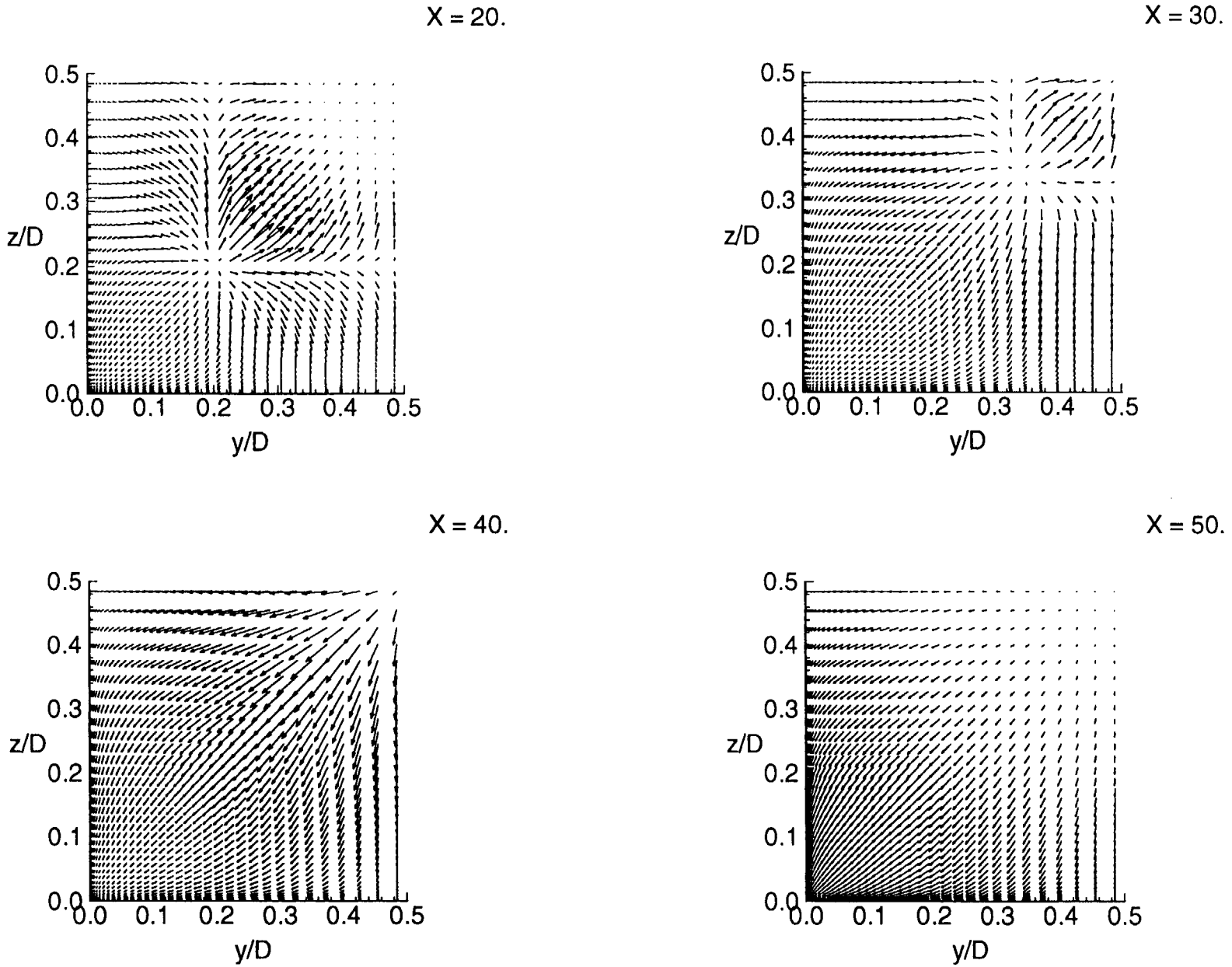

(a) Standard Jones & Launder 2-eqn. k-ε.

Figure 4. Cross-flow velocity pattern for supersonic square duct.

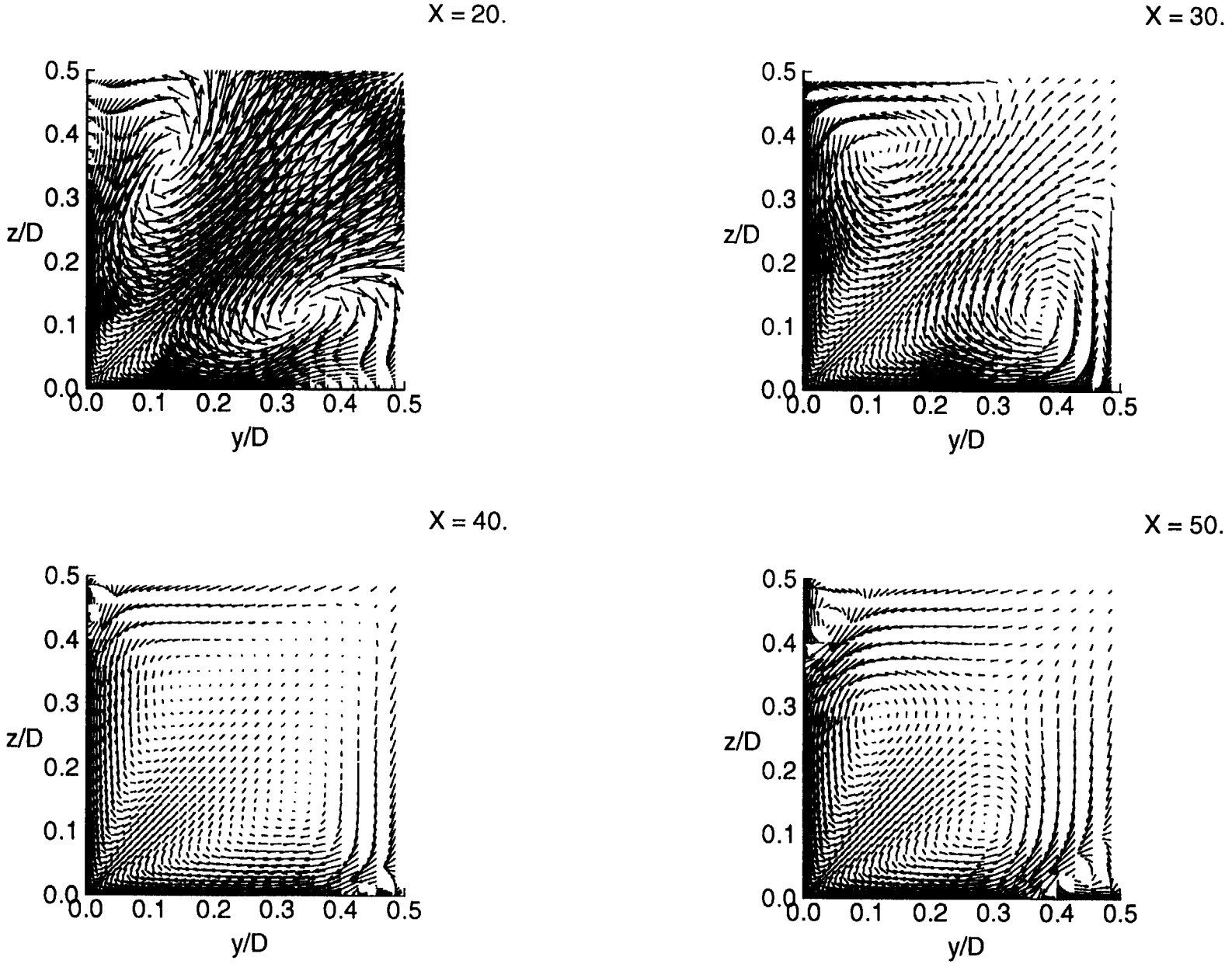

(b) Shih, Zhu & Lumley algebraic stress model

Figure 4. Concluded

REPORT DOCUMENTATION PAGE

Form Approved
OMB No. 0704-0188

1. AGENCY USE ONLY (*Leave blank*)	2. REPORT DATE	3. REPORT TYPE AND DATES COVERED
	December 1995	Contractor Report

4. TITLE AND SUBTITLE
Implementation of Algebraic Stress Models in a General 3-D Navier-Stokes Method (PAB3D)

5. FUNDING NUMBERS
C NAS1-19831
WU 505-59-30-24

6. AUTHOR(S)
Khaled S. Abdol-Hamid

7. PERFORMING ORGANIZATION NAME(S) AND ADDRESS(ES)
Analytical Services and Materials, Inc.
107 Research Drive
Hampton, VA 23666

8. PERFORMING ORGANIZATION REPORT NUMBER

9. SPONSORING / MONITORING AGENCY NAME(S) AND ADDRESS(ES)
National Aeronautics and Space Administration
Langley Research Center
Hampton, VA 23681-0001

10. SPONSORING / MONITORING AGENCY REPORT NUMBER
NASA CR-4702

11. SUPPLEMENTARY NOTES
Langley Technical Monitor: Bobby L. Berrier

12a. DISTRIBUTION / AVAILABILITY STATEMENT
Unclassified - Unlimited

Subject Category 02

12b. DISTRIBUTION CODE

13. ABSTRACT (*Maximum 200 words*)

A three-dimensional multiblock Navier-Stokes code, PAB3D, which was developed for propulsion integration and general aerodynamic analysis, has been used extensively by NASA Langley and other organizations to perform both internal (exhaust) and external flow analysis of complex aircraft configurations. This code was designed to solve the simplified Reynolds Averaged Navier-Stokes equations. A two-equation k-ε turbulence model has been used with considerable success, especially for attached flows. Accurate predicting of transonic shock wave location and pressure recovery in separated flow regions has been more difficult. Two algebraic Reynolds stress models (ASM) have been recently implemented in the code that greatly improved the code's ability to predict these difficult flow conditions. Good agreement with Direct Numerical Simulation (DNS) for a subsonic flat plate was achieved with ASMs developed by Shih, Zhu, and Lumley, and Gatski and Speziale. Good predictions were also achieved at subsonic and transonic Mach numbers for shock location and trailing edge boattail pressure recovery on a single-engine afterbody/nozzle model.

14. SUBJECT TERMS
computational fluid dynamics; Navier-Stokes, turbulence models; two-equation k-ε; algebraic reynolds stress; multiblock; separated flows, transonic flows

15. NUMBER OF PAGES
23

16. PRICE CODE
A03

17. SECURITY CLASSIFICATION OF REPORT	18. SECURITY CLASSIFICATION OF THIS PAGE	19. SECURITY CLASSIFICATION OF ABSTRACT	20. LIMITATION OF ABSTRACT
Unclassified	Unclassified	Unclassified	